Effect of gravitational wave on shadow of a Schwarzschild black hole

Mingzhi Wang[1*], Songbai Chen[2,3†], Jiliang Jing[2,3‡]
[1]*School of Mathematics and Physics, Qingdao University of Science and Technology, Qingdao, Shandong 266061, People's Republic of China*
[2]*Institute of Physics and Department of Physics, Key Laboratory of Low Dimensional Quantum Structures and Quantum Control of Ministry of Education, Synergetic Innovation Center for Quantum Effects and Applications, Hunan Normal University, Changsha, Hunan 410081, People's Republic of China*
[3]*Center for Gravitation and Cosmology, College of Physical Science and Technology, Yangzhou University, Yangzhou 225009, China*

Abstract

We have studied a shadow of a Schwarzschild black hole perturbed by gravitational wave. It is shown that the shadow changes periodically with time and it depends on the order of Legendre polynomial l and the frequency σ of gravitational wave. For the odd order of Legendre polynomial, the total shadow vibrates with time along the direction which is vertical to equatorial plane. For even l, the centre of the shadow does not move, but its shape alternately stretches and shrinks with time along the vertical direction. The deviation from Schwarzschild black hole shadow is clearer for a bigger gravitational wave frequency. Furthermore, the dispersed points and self-similar fractal structures, which are caused by chaotic lensing, appear in the boundary of the shadow for Schwarzschild black hole perturbed by gravitational wave. Our results show that gravitational wave yields a lot of interesting patterns for the black hole shadow.

PACS numbers: 04.70.Bw, 95.30.Sf, 97.60.Lf

* Corresponding author: wmz9085@126.com
† csb3752@hunnu.edu.cn
‡ jljing@hunnu.edu.cn

I. INTRODUCTION

The first direct observation of gravitational waves (GW150914)[1–3] reported by LIGO and Virgo Scientific not only confirms the success of Einstein's general relativity, but also opens a new era in the fields of astronomy, astrophysics and cosmology. Subsequently, there are several gravitational waves events have been detected, which are caused by binary black hole merger (BBH) [1–7] or by binary neutron star (BNS) merger [8]. Especially, the discovery of the electromagnetic signals in gamma-ray [8–10] arising from binary neutron star (BNS) merger means the arrival of multi-messengers astronomy. By comparing with theoretical templates, gravitational waves could tell us a variety of parameters of astrophysical compact objects such as their masses, spins and so on. The detection of gravitational waves could help us to understand further black hole and to verify various gravity theories.

Another exciting event in astrophysics and black hole physics is the first image of the supermassive black hole in the center of the giant elliptical galaxy M87, which was announced by Event Horizon Telescope Collaboration in 2019 [11–16]. It provides the first direct visual evidence that there exists exactly black hole in our Universe. Black hole image can be regarded as a potential tool to verify gravity theories and identify black hole parameters. The initial analysis of the first image of black hole has no striking deviations from the predictions of general theory of relativity. The dark region in the center of black hole image is black hole shadow, which corresponds to light rays fall into event horizon of black hole. The fingerprint of the geometry around the black hole would be reflected in the shape and size of black hole shadow[17, 18]. For example, the shadow of a Schwarzschild black hole is a perfect black disk. But for a Kerr black hole, shadow becomes a D-shaped silhouette gradually with the increase of spin parameter[17, 18]. In the spacetime of a Kerr black hole with Proca hair and a Konoplya-Zhidenko rotating non-Kerr black hole, cusp silhouette of black hole shadows emerge[19, 20]. In the spacetime of a rotating black hole with scalar hair [21–24], a Majumdar-Papapetrou binary black hole system [25, 26], Bonnor black diholes with magnetic dipole moment [27], and a non-Kerr rotating compact object with quadrupole mass moment [28], the self-similar fractal structures are found in black hole shadows which caused by non-integrable photon motions. The richer structures and patterns of black hole shadows with other parameters in various theories of gravity have been recently investigated in Refs. [29–58].

Since both the gravitational waves detection and Event Horizon Telescope observation play a vital role in the study of black holes and verification of various gravity theories, it is very interesting to study the effects of gravitational waves on black hole shadows and the change of black hole shadows with gravitational waves. In this paper, we would like to study the shadow of a Schwarzschild black hole perturbed by a special class of gravitational wave[59, 60]. This solution of gravitational wave was obtained by Xanthopoulos[59], and it satisfies the Regge-Wheeler equations. Due to the presence of gravitational wave, the equations of particle motion are no longer integrable, and then the chaotic motions for test particles appear in this background of a Schwarzschild black hole perturbed by such gravitational wave[60]. Therefore, it is expected that the chaotic lensing caused by the gravitational wave[59] would give rise to some new effects on the black hole shadow. The main purpose of this paper is to probe the features of shadow casted by a Schwarzschild black hole perturbed by the gravitational wave[59] and to detect the effects of the gravitational wave on the shadow.

The paper is organized as follows. In Sec. II, we review briefly the spacetime of a Schwarzschild black hole perturbed by gravitational wave[59, 60] and then analyze the null geodesic equations in this spacetime. In Sec. III, we present numerically the shadows for the Schwarzschild black hole perturbed by gravitational wave in different times and probe the effects of the gravitational wave on the shadow. Finally, we present a summary.

II. THE SPACETIME OF SCHWARZSCHILD BLACK HOLE PERTURBED BY GRAVITATIONAL WAVE AND NULL GEODESICS

The metric of a Schwarzschild black hole perturbed by the special class of gravitational wave[59, 60] can be described as

$$ds^2 = (g_{\mu\nu} + \epsilon h_{\mu\nu})dx^\mu dx^\nu, \tag{1}$$

where $g_{\mu\nu}$ is the metric tensor of a usual Schwarzschild black hole with a form

$$g_{tt} = -f = -(1 - 2m/r), \qquad g_{rr} = f^{-1}, \qquad g_{\theta\theta} = r^2, \qquad g_{\phi\phi} = r^2 \sin^2\theta. \tag{2}$$

$\epsilon h_{\mu\nu}$ is the perturbation from gravitational wave[59], and $h_{\mu\nu}$ is given by[59, 60]

$$\begin{aligned}
h_{tt} &= -fXP_l\cos(\sigma t), \qquad (3)\\
h_{rr} &= f^{-1}YP_l\cos(\sigma t),\\
h_{\theta\theta} &= r^2(ZP_l + W\frac{d^2P_l}{d\theta^2})\cos(\sigma t),\\
h_{\phi\phi} &= r^2\sin^2\theta(ZP_l + W\frac{dP_l}{d\theta}\cot\theta)\cos(\sigma t),
\end{aligned}$$

where

$$X = pq, \qquad Y = 3Mq, \qquad Z = (r-3M)q, \qquad W = rq, \tag{4}$$
$$p = M - \frac{M^2+\sigma^2 r^4}{r-2M}, \qquad q = \frac{\sqrt{f}}{r^2}.$$

$P_l = P_l(\cos\theta)$ are the usual Legendre polynomials($l > 1$), σ is the frequency of gravitational wave. The solution (3) is a particular solution of the first-order Einstein equations[60]. For even (odd) order l in P_l, the perturbations (3) are even (odd) functions of $\cos\theta$, therefore the gravitational wave is (not) symmetric with respect equatorial plane[59, 60]. Moreover, the spacetime of Schwarzschild black hole perturbed by gravitational wave is no static because the metric function depends on the time coordinate.

The Hamiltonian of a photon propagation along null geodesic in the spacetime of Schwarzschild black hole perturbed by gravitational wave (3) can be expressed as

$$\begin{aligned} H = \quad & -\frac{p_t^2}{2f+2\epsilon f X P_l\cos(\sigma t)} + \frac{f p_r^2}{2+2\epsilon Y P_l \cos(\sigma t)} + \frac{p_\theta^2}{2r^2[1+\epsilon(ZP_l + W\frac{d^2P_l}{d\theta^2})\cos(\sigma t)]} \\ & + \frac{\csc^2\theta p_\phi^2}{2r^2[1+\epsilon(ZP_l+W\frac{dP_l}{d\theta}\cot\theta)\cos(\sigma t)]}. \end{aligned} \tag{5}$$

We can see the Hamiltonian (5) is an explicit function of time coordinate t, and the photon moving in this spacetime only has one conserved quantity which corresponds to z component of the angular momentum

$$L_z = p_\phi = r^2\sin^2\theta[1+\epsilon(ZP_l + W\frac{dP_l}{d\theta}\cot\theta)\cos(\sigma t)]\dot{\phi}. \tag{6}$$

With the conserved quantity L_z, we can find the null geodesic equations of photon motion in the spacetime can be expressed as

$$\begin{aligned} \ddot{t} \; = \; & \frac{1}{2f\,[X\epsilon P_l\cos(\sigma t)+1]}\Bigg\{\frac{\dot{r}^2\sigma Y\epsilon P_l\sin(\sigma t)}{f} - 2\dot{r}\dot{t}\,[\epsilon P_l\,(Xf'+fX')\cos(\sigma t)+f'] - 2f\dot{\theta}\dot{t}X\epsilon\frac{dP_l}{d\theta}\cos(\sigma t) \\ & + f\sigma\dot{t}^2X\epsilon P_l\sin(\sigma t) + \frac{L_z^2\sigma\epsilon\csc^2\theta\sin(\sigma t)\left(W\cot\theta\frac{dP_l}{d\theta}+ZP_l\right)}{r^2\left[\epsilon\cos(\sigma t)\left(W\cot\theta\frac{dP_l}{d\theta}+ZP_l\right)+1\right]^2} + \dot{\theta}^2r^2\sigma\epsilon\sin(\sigma t)\left(W\frac{d^2P_l}{d\theta^2}+ZP_l\right)\Bigg\}, \end{aligned} \tag{7}$$

$$\begin{aligned} \ddot{r} \; = \; & \frac{f}{2\,[Y\epsilon P_l\cos(\sigma t)+1]}\Bigg\{-\dot{t}^2\,[\epsilon P_l\,(Xf'+fX')\cos(\sigma t)+f'] + \frac{\dot{r}^2\,[\epsilon P_l\,(Yf'-fY')\cos(\sigma t)+f']}{f^2} \\ & + \frac{2\dot{r}\sigma\dot{t}Y\epsilon P_l\sin(\sigma t)}{f} + \frac{L_z^2\csc^2\theta\{\epsilon\cos(\sigma t)\left[\cot\theta\,(rW'+2W)\frac{dP_l}{d\theta}+P_l\,(rZ'+2Z)\right]+2\}}{r^3\left[\epsilon\cos(\sigma t)\left(W\cot\theta\frac{dP_l}{d\theta}+ZP_l\right)+1\right]^2} \\ & + \dot{\theta}^2r\Bigg\{\epsilon\cos(\sigma t)\left[(rW'+2W)\frac{d^2P_l}{d\theta^2}+P_l\,(rZ'+2Z)\right]+2\Bigg\} - \frac{2\dot{\theta}\dot{r}Y\epsilon\frac{dP_l}{d\theta}\cos(\sigma t)}{f}\Bigg\}, \end{aligned} \tag{8}$$

$$\ddot{\theta} = \frac{1}{2r^2\left[\epsilon\cos(\sigma t)\left(W\frac{d^2P_l}{d\theta^2}+ZP_l\right)+1\right]}\left\{\frac{\dot{r}^2Y\epsilon\frac{dP_l}{d\theta}\cos(\sigma t)}{f}+\dot{\theta}^2r^2\epsilon\cos(\sigma t)\left(W\frac{d^3P_l}{d\theta^3}+Z\frac{dP_l}{d\theta}\right)\right. \tag{9}$$
$$+\frac{L_z^2\csc^2\theta\left\{2\cot\theta+\epsilon\cos(\sigma t)\left[W\left(\cot^2\theta-1\right)\frac{dP_l}{d\theta}+W\cot\theta\frac{d^2P_l}{d\theta^2}+Z\left(2\cot\theta P_l+\frac{dP_l}{d\theta}\right)\right]\right\}}{r^2\left[\epsilon\cos(\sigma t)\left(W\cot\theta\frac{dP_l}{d\theta}+ZP_l\right)+1\right]^2}$$
$$+2\dot{\theta}r^2\sigma\dot{t}\epsilon\sin(\sigma t)\left(W\frac{d^2P_l}{d\theta^2}+ZP_l\right)-2\dot{\theta}\dot{r}r\left(\epsilon\cos(\sigma t)\left(\frac{d^2P_l}{d\theta^2}\left(rW'+2W\right)+P_l\left(rZ'+2Z\right)\right)+2\right)$$
$$\left.-f\dot{t}^2X\epsilon\frac{dP_l}{d\theta}\cos(\sigma t)\right\},$$

$$\dot{\phi} = \frac{L_z\csc^2\theta}{r^2[1+\epsilon(ZP_l+W\frac{dP_l}{d\theta}\cot\theta)\cos(\sigma t)]}, \tag{10}$$

where the dots denote derivatives with respect to the proper time τ, and the primes denote derivatives with respect to the radial coordinate r. It is obvious that the photon dynamical system is non-integrable, so the motion of photon could be chaotic in this spacetime.

III. SHADOWS CASTED BY SCHWARZSCHILD BLACK HOLE PERTURBED BY GRAVITATIONAL WAVE

In this section, we will study the shadows of Schwarzschild black hole perturbed by gravitational wave with the backward ray-tracing technique [21–30]. We evolved light rays by solving numerically the null geodesic equations (7) from the observer backward in time and can obtain the information carried by each ray. The shadow of black hole is composed by the light rays falling down into the horizon of black hole. Since the perturbations from gravitational wave at spatial infinity are negligible, the spacetime of Schwarzschild black hole perturbed by gravitational wave is asymptotically flat. We can define the observer's sky as the usual cases in which the observer basis $\{e_{\hat{t}}, e_{\hat{r}}, e_{\hat{\theta}}, e_{\hat{\phi}}\}$ can be expanded as a form in the coordinate basis $\{\partial_t, \partial_r, \partial_\theta, \partial_\phi\}$ [21–30]

$$e_{\hat{\mu}} = e^{\nu}_{\hat{\mu}}\partial_\nu, \tag{11}$$

where the transform matrix $e^{\nu}_{\hat{\mu}}$ obeys $(g_{\mu\nu}+\epsilon h_{\mu\nu})e^{\mu}_{\hat{\alpha}}e^{\nu}_{\hat{\beta}} = \eta_{\hat{\alpha}\hat{\beta}}$, and $\eta_{\hat{\alpha}\hat{\beta}}$ is the Minkowski metric. It is convenient to choice a decomposition as

$$e^{\nu}_{\hat{\mu}} = \begin{pmatrix} \frac{1}{\sqrt{-g_{tt}-\epsilon h_{tt}}} & 0 & 0 & 0 \\ 0 & \frac{1}{\sqrt{g_{rr}+\epsilon h_{rr}}} & 0 & 0 \\ 0 & 0 & \frac{1}{\sqrt{g_{\theta\theta}+\epsilon h_{\theta\theta}}} & 0 \\ 0 & 0 & 0 & \frac{1}{\sqrt{g_{\phi\phi}+\epsilon h_{\phi\phi}}} \end{pmatrix}. \tag{12}$$

Thus the locally measured four-momentum $p^{\hat{\mu}}$ of a photon can be obtained through the projection of its four-momentum p^{μ} onto $e_{\hat{\mu}}$, i.e.,

$$\begin{aligned}
p^{\hat{t}} &= -e^{\nu}_{\hat{t}} p_{\nu} = -\frac{1}{\sqrt{f+\epsilon f X P_l \cos(\sigma t)}} p_t, \\
p^{\hat{r}} &= e^{\nu}_{\hat{r}} p_{\nu} = \sqrt{\frac{f}{1+\epsilon Y P_l \cos(\sigma t)}} p_r, \\
p^{\hat{\theta}} &= e^{\nu}_{\hat{\theta}} p_{\nu} = \frac{1}{\sqrt{1+\epsilon(Z P_l + W\frac{d^2 P_l}{d\theta^2})\cos(\sigma t)}} \frac{p_\theta}{r}, \\
p^{\hat{\phi}} &= e^{\nu}_{\hat{\phi}} p_{\nu} = \frac{1}{\sqrt{1+\epsilon(Z P_l + W\frac{d P_l}{d\theta}\cot\theta)\cos(\sigma t)}} \frac{L_z \csc\theta}{r}.
\end{aligned} \tag{13}$$

After the similar processes in Refs.[21–30], one can obtain the coordinates of a photon's image in observer's sky

$$\begin{aligned}
x &= -r\frac{p^{\hat{\phi}}}{p^{\hat{r}}}|_{(r_{obs},\theta_{obs})} = -\sqrt{\frac{f}{[1+\epsilon(Z P_l + W\frac{d P_l}{d\theta}\cot\theta)\cos(\sigma t)][1+\epsilon Y P_l\cos(\sigma t)]}} \frac{L_z\csc\theta}{\dot{r}}|_{(r_{obs},\theta_{obs})}, \\
y &= r\frac{p^{\hat{\theta}}}{p^{\hat{r}}}|_{(r_{obs},\theta_{obs})} = \sqrt{\frac{f[1+\epsilon(Z P_l + W\frac{d^2 P_l}{d\theta^2})\cos(\sigma t)]}{1+\epsilon Y P_l \cos(\sigma t)}} \frac{r^2\dot{\theta}}{\dot{r}}|_{(r_{obs},\theta_{obs})},
\end{aligned} \tag{14}$$

where the spatial position of observer is set at (r_{obs}, θ_{obs}).

In Fig.1-4, we present the shadows of Schwarzschild black hole with different gravitational waves which observer obtain at different times t_{obs}. Here, we set the observer at $r_{obs} = 50$, $\theta_{obs} = 90°$ (the observer locates at the equatorial plane of the black hole), and the mass of Schwarzschild black hole $M = 1$. From Fig.1 and Fig.2, we can see the shadows of Schwarzschild black hole perturbed by gravitational wave are similar with the circular shadow of Schwarzschild black hole. But our further calculations indicate the total shadow vibrates with time along the direction which is vertical to equatorial plane for odd l. For even l, the centre of the shadow does not move, but its shape alternately stretches and shrinks with time along the vertical direction. Moreover, similar to the symmetry of gravitational wave, the shadows of Schwarzschild black hole perturbed by gravitational wave are (not) symmetric with respect equatorial plane for even (odd) l. The changes of shadows casted by Schwarzschild black hole with gravitational wave are clearer in Fig.3 and Fig.4, where $\epsilon = 0.05$ and gravitational wave frequency $\sigma = 0.2$, 0.5 respectively. Furthermore, the shadows have more distinct deformations than those in the cases in Figs.1-2. It is obvious that there exist the drop-like shaped shadows in the case of $l = 3$ and the stretching or contracting shadows in the case of $l = 4$. From these shadows we can find the shadow of Schwarzschild black hole perturbed by gravitational wave is not static but changes periodically. In addition, we zoom in the area within the red box in Fig.4(g), and find that there exist dispersed points and self-similar fractal structures in the boundary of shadow, which is shown in Fig.5. Their

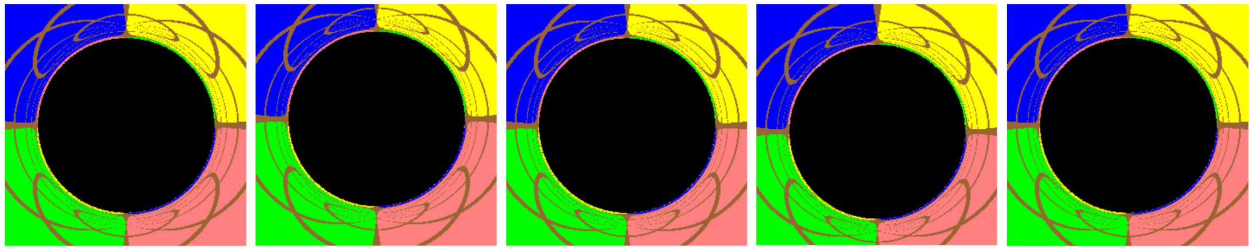

(a)$l = 3, t_{obs} = 0$ (b)$l = 3, t_{obs} = \frac{\pi}{2}$ (c)$l = 3, t_{obs} = \pi$ (d)$l = 3, t_{obs} = \frac{3\pi}{2}$ (e)$l = 3, t_{obs} = 2\pi$

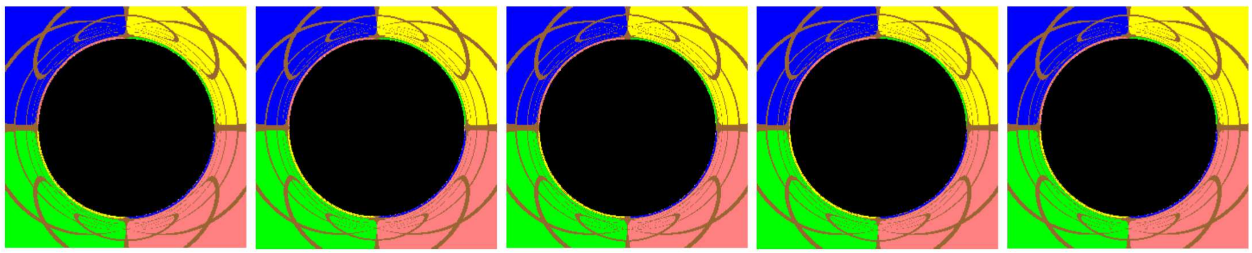

(f)$l = 4, t_{obs} = 0$ (g)$l = 4, t_{obs} = \frac{\pi}{2}$ (h)$l = 4, t_{obs} = \pi$ (i)$l = 4, t_{obs} = \frac{3\pi}{2}$ (j)$l = 4, t_{obs} = 2\pi$

FIG. 1: The shadows of Schwarzschild black hole perturbed by gravitational wave at different times t_{obs}. Here we set mass $M = 1$, $\epsilon = 0.01$, gravitational wave frequency $\sigma = 1$, $l = 3$ in the upper row, $l = 4$ in the lower row, and the observer is set at $r_{obs} = 50$ with the inclination angle $\theta_{obs} = 90^\circ$.

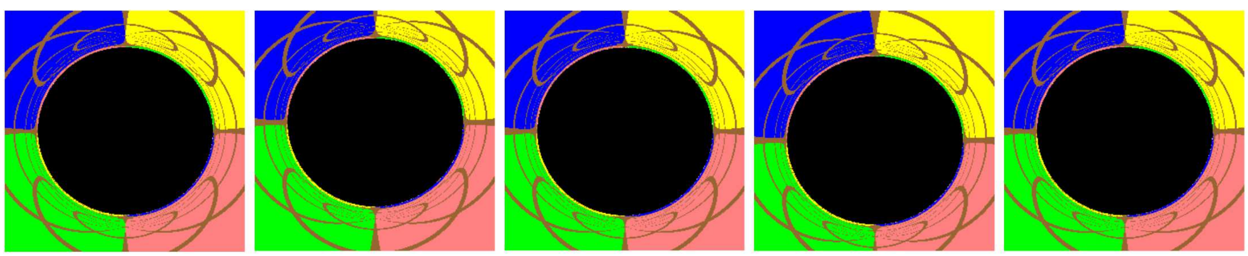

(a)$l = 3, t_{obs} = 0$ (b)$l = 3, t_{obs} = \frac{5\pi}{14}$ (c)$l = 3, t_{obs} = \frac{5\pi}{7}$ (d)$l = 3, t_{obs} = \frac{15\pi}{14}$ (e)$l = 3, t_{obs} = \frac{20\pi}{14}$

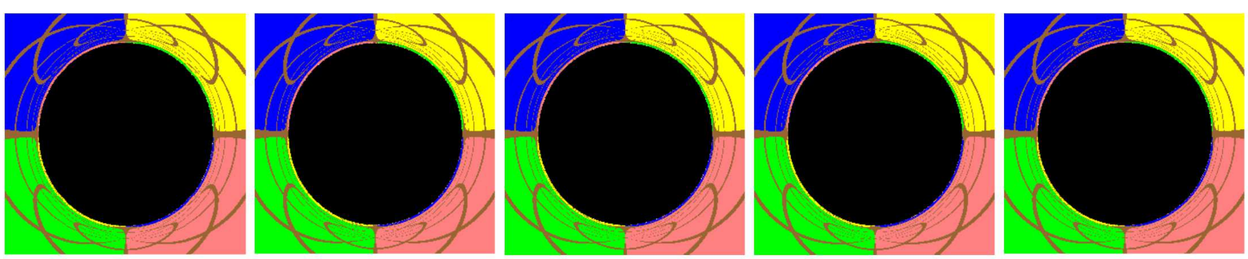

(f)$l = 4, t_{obs} = 0$ (g)$l = 4, t_{obs} = \frac{5\pi}{14}$ (h)$l = 4, t_{obs} = \frac{5\pi}{7}$ (i)$l = 4, t_{obs} = \frac{15\pi}{14}$ (j)$l = 4, t_{obs} = \frac{20\pi}{14}$

FIG. 2: The shadows of Schwarzschild black hole perturbed by gravitational waves at different times t_{obs}. Here we set mass $M = 1$, $\epsilon = 0.01$, gravitational waves frequency $\sigma = 1.4$, $l = 3$ in the upper row, $l = 4$ in the lower row, and the observer is set at $r_{obs} = 50$ with the inclination angle $\theta_{obs} = 90^\circ$.

appearance hints there are chaos in shadows of Schwarzschild black hole perturbed by the gravitational wave.

In order to study quantitatively the deformation for the black hole shadow perturbed by the gravitational wave (3), we calculated two deviated parameters ε_o and ε_e, which measure the deviation of these shadows from usual Schwarzschild black hole shadow. Considering that the parity of l in Legendre polynomials p_l give rise to different effects of gravitational wave (3) on shadow of Schwarzschild black hole, we set the deviated

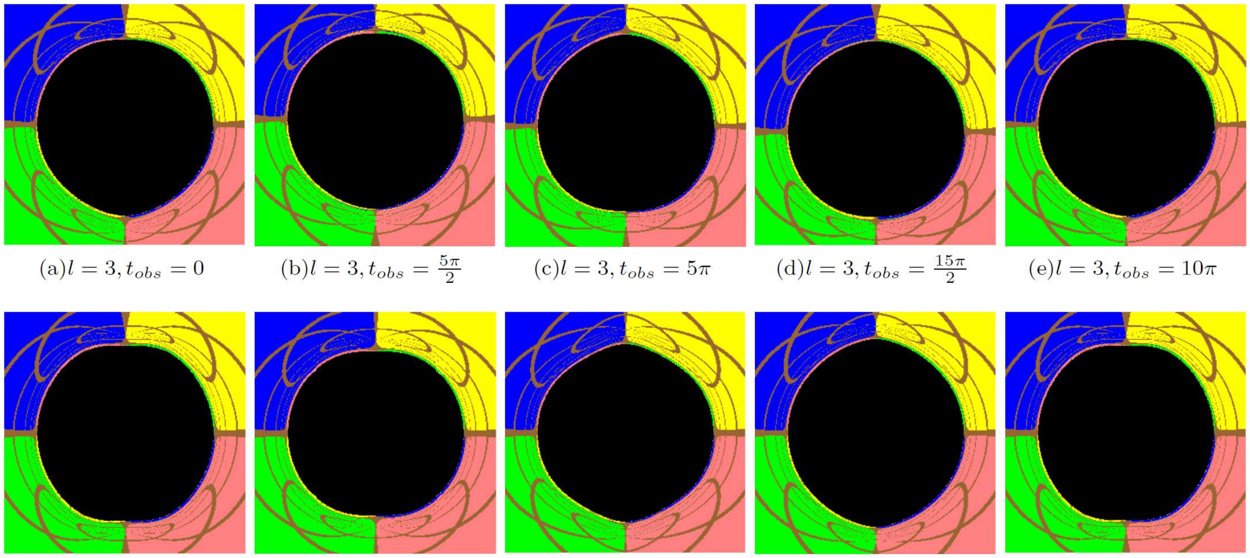

(a)$l = 3, t_{obs} = 0$ (b)$l = 3, t_{obs} = \frac{5\pi}{2}$ (c)$l = 3, t_{obs} = 5\pi$ (d)$l = 3, t_{obs} = \frac{15\pi}{2}$ (e)$l = 3, t_{obs} = 10\pi$

(f)$l = 4, t_{obs} = 0$ (g)$l = 4, t_{obs} = \frac{5\pi}{2}$ (h)$l = 4, t_{obs} = 5\pi$ (i)$l = 4, t_{obs} = \frac{15\pi}{2}$ (j)$l = 4, t_{obs} = 10\pi$

FIG. 3: The shadows of Schwarzschild black hole perturbed by gravitational wave at different times t_{obs}. Here we set mass $M = 1$, $\epsilon = 0.05$, gravitational wave frequency $\sigma = 0.2$, $l = 3$ in the upper row, $l = 4$ in the lower row, and the observer is set at $r_{obs} = 50$ with the inclination angle $\theta_{obs} = 90^{\circ}$.

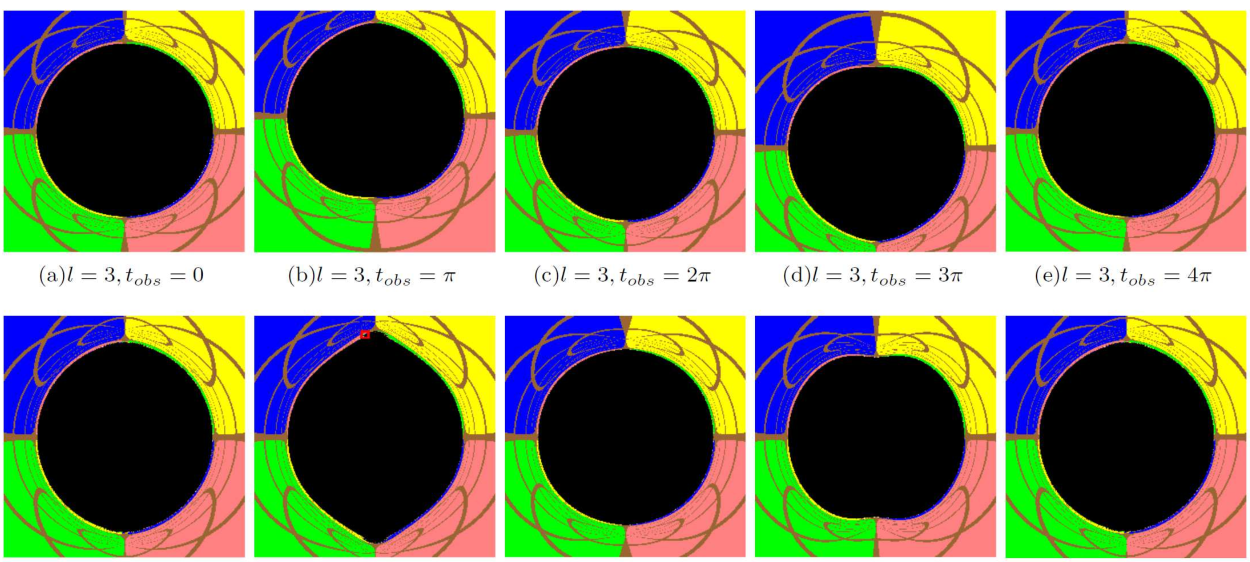

(a)$l = 3, t_{obs} = 0$ (b)$l = 3, t_{obs} = \pi$ (c)$l = 3, t_{obs} = 2\pi$ (d)$l = 3, t_{obs} = 3\pi$ (e)$l = 3, t_{obs} = 4\pi$

(f)$l = 4, t_{obs} = 0$ (g)$l = 4, t_{obs} = \pi$ (h)$l = 4, t_{obs} = 2\pi$ (i)$l = 4, t_{obs} = 3\pi$ (j)$l = 4, t_{obs} = 4\pi$

FIG. 4: The shadows of Schwarzschild black hole perturbed by gravitational wave at different times t_{obs}. Here we set mass $M = 1$, $\epsilon = 0.05$, gravitational wave frequency $\sigma = 0.5$, $l = 3$ in the upper row, $l = 4$ in the lower row, and the observer is set at $r_{obs} = 50$ with the inclination angle $\theta_{obs} = 90^{\circ}$.

parameters ε_o and ε_e to measure the deviation of shadows for odd l and even l, respectively. As l is odd, the deviated parameter ε_o can be expressed as

$$\varepsilon_o = \frac{y_t + y_b}{r_S}, \tag{15}$$

where y_t is the y coordinate of the topmost point in shadow, y_b is the y coordinate of the bottommost point in shadow, and r_S is the radius of Schwarzschild black hole shadow. If black hole shadow shifts upward

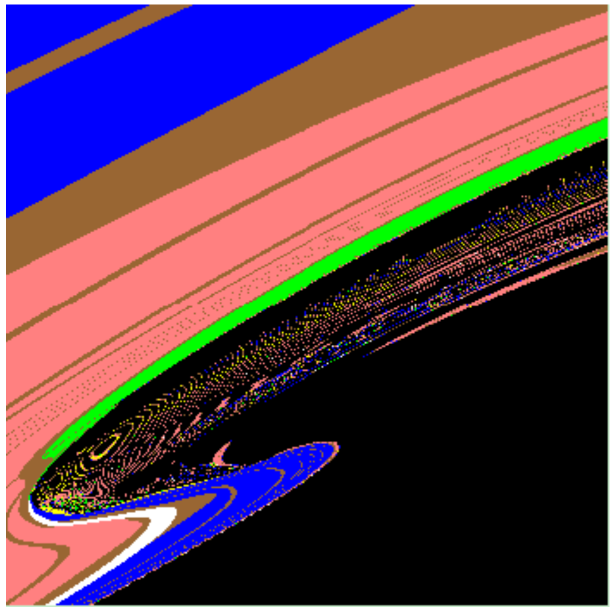

FIG. 5: The amplifying image of the area within the red box in Fig.4(g).

(downward), the deviated parameter ε_o will greater than zero (less than zero). As l is even, since the shadow alternately stretches and shrinks along the vertical direction, and then the deviated parameter ε_e can be expressed as

$$\varepsilon_e = \frac{y_t}{x_r} - 1, \tag{16}$$

where x_r is the x coordinate of the rightmost point in shadow. If black hole shadow is prolate (oblate) than Schwarzschild black hole shadow, the deviated parameter ε_e will greater than zero (less than zero). In Fig.6 and Fig.7, we show the changes of the deviated parameters ε_o for $l = 3$ and ε_e for $l = 4$ with time t_{obs}. We found the deviated parameter ε_o fluctuates up and down with time for $\epsilon = 0.01$, $l = 3$ and $\sigma = 1$, 1.4 in Fig.6(a). What's more, the amplitude of the deviated parameter ε_o is larger for a bigger gravitational wave frequency σ. From Fig.7(a) we can find the similar situation for $\epsilon = 0.05$, $l = 3$, and $\sigma = 0.2$, 0.5. In Fig.6(b), the deviated parameter ε_e is always greater than zero for $\epsilon = 0.01$, $l = 4$, and $\sigma = 1$, 1.4 , which indicates that the shadows in this case are always prolate than Schwarzschild black hole shadow. But we can find ε_e fluctuates slightly and the prolateness of shadow changes periodically with time. Moreover, the prolateness of shadow increases with increase of the gravitational wave frequency σ. For the case $\epsilon = 0.05$, $l = 4$, and $\sigma = 0.2$, 0.5, as shown in Fig.7(b), the deviated parameter ε_e fluctuates up and down around zero, which means the shadow is alternately prolate and oblate than Schwarzschild black hole shadow with time.

It is necessary to study the shadows that observer obtain at other inclination angles θ_{obs}. In Fig.8 and Fig.9, we show the shadows for the observers at inclination angle $\theta_{obs} = 0°$ and $45°$ in different times t_{obs}. Here

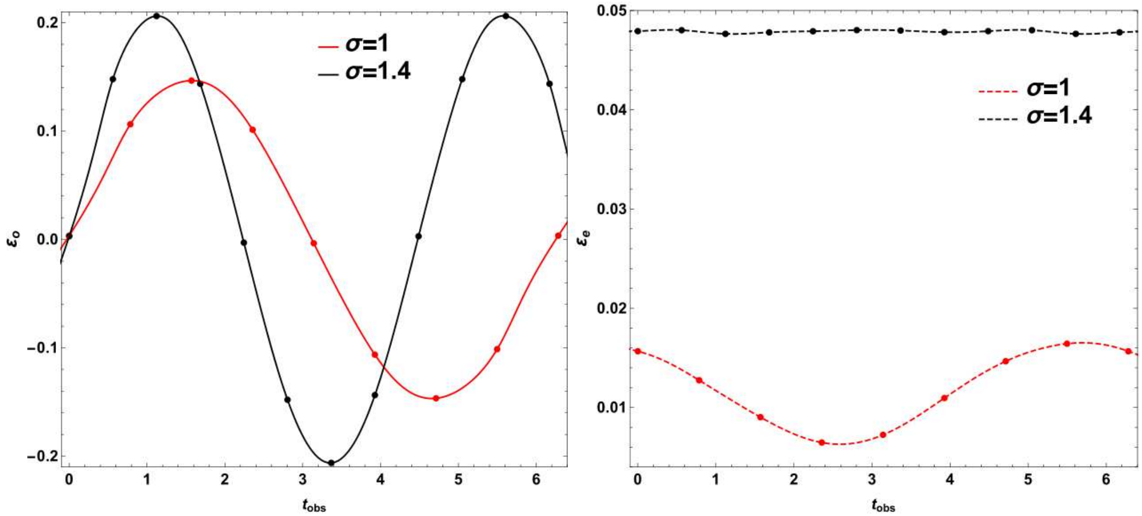

(a)$l = 3$ (b)$l = 4$

FIG. 6: The changes of the deviated parameters ε_o for $l = 3$ and ε_e for $l = 4$ with time t_{obs}. Here we set $\epsilon = 0.01$ and gravitational wave frequency $\sigma = 1$, 1.4.

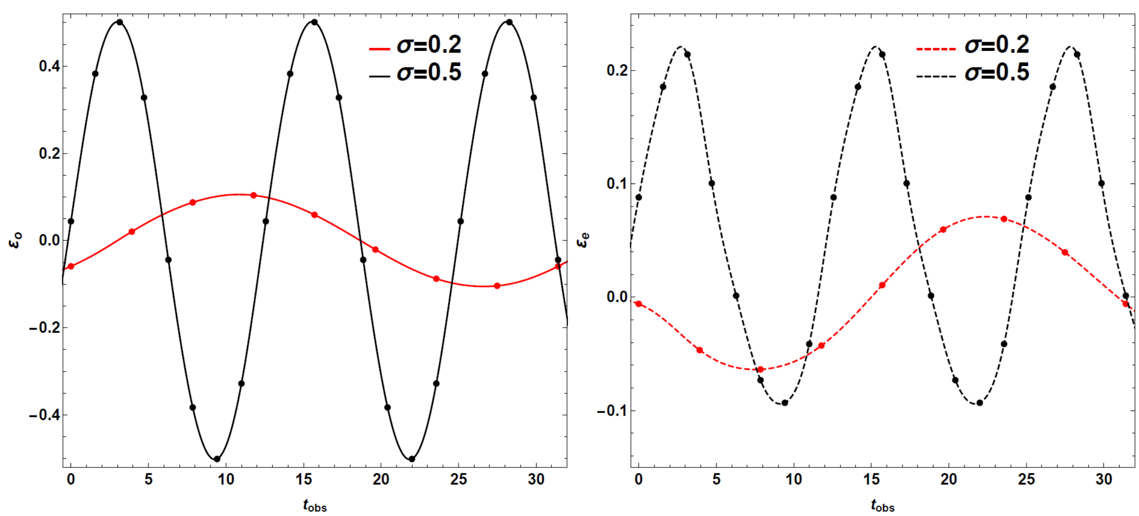

(a)$l = 3$ (b)$l = 4$

FIG. 7: The changes of the deviated parameters ε_o for $l = 3$ and ε_e for $l = 4$ with time t_{obs}. Here we set $\epsilon = 0.05$ and gravitational wave frequency $\sigma = 0.2$, 0.5.

we set $\epsilon = 0.05$, gravitational wave frequency $\sigma = 0.5$, and $l = 3$, 4 respectively. We found when inclination angle $\theta_{obs} = 0°$ the shadows of Schwarzschild black hole perturbed by gravitational wave alternately expand and contract with time. When inclination angle $\theta_{obs} = 45°$, the shadows vibrate with time along the vertical direction with time for $l = 3$ as shown in Fig.8, and they are no longer symmetric with respect the equatorial plane for $l = 4$ as shown in Fig.9.

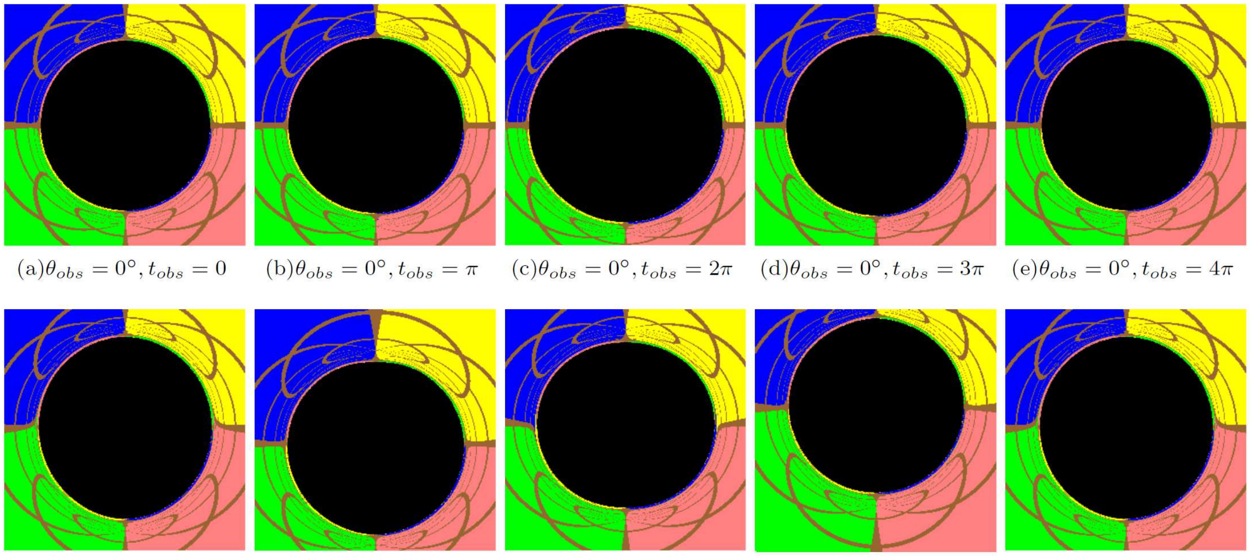

(a)$\theta_{obs} = 0°, t_{obs} = 0$ (b)$\theta_{obs} = 0°, t_{obs} = \pi$ (c)$\theta_{obs} = 0°, t_{obs} = 2\pi$ (d)$\theta_{obs} = 0°, t_{obs} = 3\pi$ (e)$\theta_{obs} = 0°, t_{obs} = 4\pi$

(f)$\theta_{obs} = 45°, t_{obs} = 0$ (g)$\theta_{obs} = 45°, t_{obs} = \pi$ (h)$\theta_{obs} = 45°, t_{obs} = 2\pi$ (i)$\theta_{obs} = 45°, t_{obs} = 3\pi$ (j)$\theta_{obs} = 45°, t_{obs} = 4\pi$

FIG. 8: The shadows for the observers at inclination angle $\theta_{obs} = 0°$ and $45°$ in different times t_{obs}, and we set $\epsilon = 0.05$, gravitational wave frequency $\sigma = 0.5$, $l = 3$.

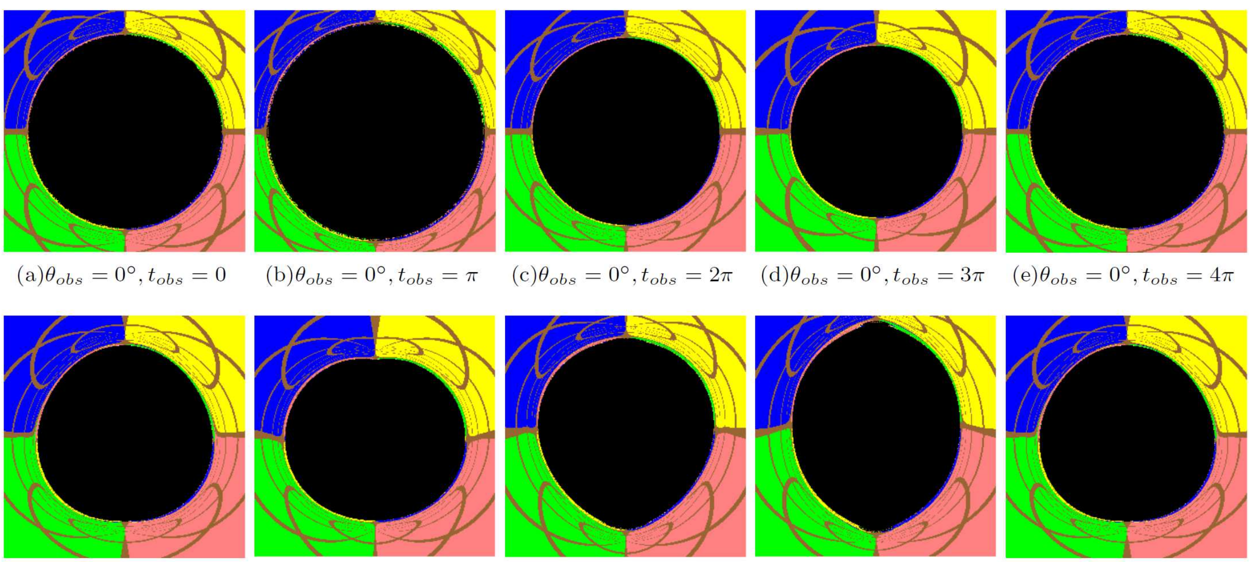

(a)$\theta_{obs} = 0°, t_{obs} = 0$ (b)$\theta_{obs} = 0°, t_{obs} = \pi$ (c)$\theta_{obs} = 0°, t_{obs} = 2\pi$ (d)$\theta_{obs} = 0°, t_{obs} = 3\pi$ (e)$\theta_{obs} = 0°, t_{obs} = 4\pi$

(f)$\theta_{obs} = 45°, t_{obs} = 0$ (g)$\theta_{obs} = 45°, t_{obs} = \pi$ (h)$\theta_{obs} = 45°, t_{obs} = 2\pi$ (i)$\theta_{obs} = 45°, t_{obs} = 3\pi$ (j)$\theta_{obs} = 45°, t_{obs} = 4\pi$

FIG. 9: The shadows for the observers at inclination angle $\theta_{obs} = 0°$ and $45°$ in different times t_{obs}, and we set $\epsilon = 0.05$, gravitational wave frequency $\sigma = 0.5$, $l = 4$.

IV. SUMMARY

In this paper we studied a shadow of a Schwarzschild black hole perturbed by a special class of gravitational wave. Under the influence of gravitational wave, the equations of photon motion in this spacetime are no longer integrable, and the shadow changes periodically. When the order of Legendre polynomial l is odd, the total shadow vibrates with time along the direction which is vertical to equatorial plane. When l is even, the centre of the shadow does not move, but its shape alternately stretches and shrinks with time along the vertical direction. We studied the effects of gravitational wave on Schwarzschild black hole shadows by calculating two deviated parameters ε_o and ε_e in different times, and found the deviation from Schwarzschild black hole shadow is clearer for a bigger gravitational wave frequency σ. We also found that there exist dispersed points and self-similar fractal structures in the boundary of shadows, which indicates that chaos appear in the shadows of Schwarzschild black hole perturbed by the gravitational wave. In addition, we present the shadows for the observer locating at inclination angle $\theta_{obs} = 0°$ and $45°$, respectively. Our results show that gravitational wave yields a lot of interesting patterns for the black hole shadow.

V. ACKNOWLEDGMENTS

This work was partially supported by the National Natural Science Foundation of China under Grant No. 11875026, the Scientific Research Fund of Hunan Provincial Education Department Grant No. 17A124. J. Jing's work was partially supported by the National Natural Science Foundation of China under Grant No. 11475061, 11875025.

[1] B. P. Abbott et al. (LIGO Scientific Collaboration and Virgo Collaboration), *Observation of Gravitational Waves from a Binary Black Hole Merger*, Phys. Rev. Lett. **116**, 061102 (2016).

[2] B. P. Abbott et al. (LIGO Scientific Collaboration and Virgo Collaboration), *GW150914: The Advanced LIGO Detectors in the Era of First Discoveries*, Phys. Rev. Lett. **116**, 131103 (2016).

[3] B. P. Abbott et al. (LIGO Scientific Collaboration and Virgo Collaboration), *GW150914: First results from the search for binary black hole coalescence with Advanced LIGO*, Phys. Rev. D. **93**, 122003 (2016).

[4] B. P. Abbott et al. [LIGO Scientific Collaboration and Virgo Collaboration], *GW151226: Observation of Gravitational Waves from a 22-Solar-Mass Binary Black Hole Coalescence*, Phys. Rev. Lett. **116**, 241103 (2016).

[5] B. P. Abbott et al. [LIGO Scientific Collaboration and Virgo Collaboration], *GW170104: Observation of a 50-Solar-Mass Binary Black Hole Coalescence at Redshift 0.2*, Phys. Rev. Lett. **118**, 221101 (2017).

[6] B. P. Abbott et al. [LIGO Scientific Collaboration and Virgo Collaboration], *GW170608: Observation of a 19 solar-mass binary black hole coalescence*, Astrophys. J. **851**, L35 (2017).

[7] B. P. Abbott et al. [LIGO Scientific Collaboration and Virgo Collaboration], *GW170814: A Three-Detector Observation of Gravitational Waves from a Binary Black Hole Coalescence*, Phys. Rev. Lett. **119**, 141101 (2017).

[8] B. P. Abbott et al. [LIGO Scientific Collaboration and Virgo Collaboration], *GW170817: Observation of Gravitational Waves from a Binary Neutron Star Inspiral*, Phys. Rev. Lett. **119**, 161101 (2017).

[9] A. Goldstein et al., *An Ordinary Short Gamma-Ray Burst with Extraordinary Implications: Fermi-GBM Detection of GRB 170817A*, Astrophys. J. **848**, L14 (2017).

[10] V. Savchenko et al., *INTEGRAL Detection of the First Prompt Gamma-Ray Signal Coincident with the Gravitational-wave Event GW170817*, Astrophys. J. **848**, L15 (2017).

[11] The Event Horizon Telescope Collaboration, *First M87 Event Horizon Telescope Results. I. The Shadow of the Supermassive Black Hole*, Astrophys. J. Lett. **875**, L1 (2019).

[12] The Event Horizon Telescope Collaboration, *First M87 Event Horizon Telescope Results. II. Array and Instrumentation*, Astrophys. J. Lett. **875**, L2 (2019).

[13] The Event Horizon Telescope Collaboration, *First M87 Event Horizon Telescope Results. III. Data Processing and Calibration*, Astrophys. J. Lett. **875**, L3 (2019).

[14] The Event Horizon Telescope Collaboration, *First M87 Event Horizon Telescope Results. IV. Imaging the Central Supermassive Black Hole*, Astrophys. J. Lett. **875**, L4 (2019).

[15] The Event Horizon Telescope Collaboration, *First M87 Event Horizon Telescope Results. V. Physical Origin of the Asymmetric Ring*, Astrophys. J. Lett. **875**, L5 (2019).

[16] The Event Horizon Telescope Collaboration, *First M87 Event Horizon Telescope Results. VI. The Shadow and Mass of the Central Black Hole*, Astrophys. J. Lett. **875**, L6 (2019).

[17] J. M. Bardeen, *Timelike and null geodesics in the Kerr metric*, in *Black Holes (Les Astres Occlus)*, edited by C. DeWitt and B. DeWitt (Gordon and Breach, New York, 1973), p. 215-239.

[18] S. Chandrasekhar, *The Mathematical Theory of Black Holes* (Oxford University Press, New York, 1992).

[19] P. V. P. Cunha, C. Herdeiro, and E. Radu, *Fundamental photon orbits: black hole shadows and spacetime instabilities*, Phys. Rev. D **96**, 024039 (2017).

[20] M. Wang, S. Chen, J. Jing, *Shadow casted by a Konoplya-Zhidenko rotating non-Kerr black hole*, J. Cosmol. Astropart. Phys. **10**, 051 (2017).

[21] P. V. P. Cunha, C. Herdeiro, E. Radu and H. F. Runarsson, *Shadows of Kerr black holes with scalar hair*, Phys. Rev. Lett. **115**, 211102 (2015), arXiv:1509.00021.

[22] P. V. P. Cunha, C. Herdeiro, E. Radu and H. F. Runarsson, *Shadows of Kerr black holes with and without scalar hair*, Int. J. Mod. Phys. D **25**, 1641021 (2016), arXiv:1605.08293.

[23] F. H. Vincent, E. Gourgoulhon, C. Herdeiro and E. Radu, *Astrophysical imaging of Kerr black holes with scalar hair*, Phys. Rev. D **94**, 084045 (2016), arXiv:1606.04246.

[24] P. V. P. Cunha, J. Grover, C. Herdeiro, E. Radu, H. Runarsson, and A. Wittig, *Chaotic lensing around boson stars and Kerr black holes with scalar hair*, Phys. Rev. D **94**, 104023 (2016).

[25] J. O. Shipley, and S. R. Dolan, *Binary black hole shadows, chaotic scattering and the Cantor set*, Class. Quantum Grav. **33**, 175001 (2016).

[26] A. Bohn, W. Throwe, F. Hbert, K. Henriksson, and D. Bunandar, *What does a binary black hole merger look like?*, Class. Quantum Grav. **32**, 065002 (2015), arXiv: 1410.7775.

[27] M. Wang, S. Chen, J. Jing, *Shadows of Bonnor black dihole by chaotic lensing*, Phys. Rev. D **97**, 064029 (2018).

[28] M. Wang, S. Chen, J. Jing, *Chaotic shadow of a non-Kerr rotating compact object with quadrupole mass moment*, Phys. Rev. D **98**, 104040 (2018).

[29] T. Johannsen, *Photon Rings around Kerr and Kerr-like Black Holes*, Astrophys. J. **777**, 170, (2013).

[30] M. Wang, S. Chen, J. Wang, J. Jing, *Shadow of a Schwarzschild black hole surrounded by a Bach-Weyl ring*, arXiv:1904.12423v1.

[31] H. Falcke, F. Melia, and E. Agol, *Viewing the Shadow of the Black Hole at the Galactic Center*, Astrophys. J. **528**, L13 (2000), arXiv: 9912263.

[32] A. de Vries, *The apparent shape of a rotating charged black hole, closed photon orbits and the bifurcation set A_4*,

Class. Quant. Grav. **17**,123 (2000).

[33] R. Takahashi, *Shapes and Positions of Black Hole Shadows in Accretion Disks and Spin Parameters of Black Holes*, Astrophys. J. **611**, 996 (2004), arXiv: 0405099.

[34] C. Bambi and K. Freese, *Apparent shape of super-spinning black holes*, Phys. Rev. D **79**, 043002 (2009), arXiv:0812.1328.

[35] Z. Li and C. Bambi, *Measuring the Kerr spin parameter of regular black holes from their shadow*, J. Cosmol. Astropart. Phys. **1401**, 041(2014),arXiv:1309.1606.

[36] K. Hioki and K. I. Maeda, *Measurement of the Kerr Spin Parameter by Observation of a Compact Object's Shadow*, Phys. Rev. D **80**, 024042 (2009), arXiv:0904.3575.

[37] L. Amarilla, E. F. Eiroa, and G. Giribet, *Null geodesics and shadow of a rotating black hole in extended Chern-Simons modified gravity*, Phys. Rev. D **81**, 124045 (2010), arXiv:1005.0607.

[38] L. Amarilla and E. F. Eiroa, *Shadow of a rotating braneworld black hole*, Phys. Rev. D **85**, 064019 (2012), arXiv:1112.6349.

[39] E. F. Eiroa and ,C. M. Sendra, *Shadow cast by rotating braneworld black holes with a cosmological constant*, Eur. Phys. J. C **78**, 91 (2018), arXiv:1711.08380.

[40] A. Yumoto, D. Nitta, T. Chiba, and N. Sugiyama,*Shadows of Multi-Black Holes: Analytic Exploration*, Phys. Rev. D **86**, 103001 (2012), arXiv:1208.0635.

[41] L. Amarilla and E. F. Eiroa, *Shadow of a Kaluza-Klein rotating dilaton black hole*, Phys. Rev. D **87**, 044057 (2013), arXiv:1301.0532.

[42] P. G. Nedkova, V. Tinchev, and S. S. Yazadjiev, *The Shadow of a Rotating Traversable Wormhole*, Phys. Rev. D **88**, 124019 arXiv:1307.7647.

[43] V. K. Tinchev and S. S. Yazadjiev, *Possible imprints of cosmic strings in the shadows of galactic black holes*, Int. J. Mod. Phys. D **23**, 1450060 (2014), arXiv:1311.1353.

[44] S. W. Wei and Y. X. Liu,*Observing the shadow of Einstein-Maxwell-Dilaton-Axion black hole*, J. Cosmol. Astropart. Phys. **11**, 063 (2013).

[45] V. Perlick, O. Y. Tsupko, and G. S. Bisnovatyi-Kogan, *Influence of a plasma on the shadow of a spherically symmetric black hole*, Phys. Rev. D **92**, 104031 (2015).

[46] Y. Huang, S. Chen, and J. Jing, *Double shadow of a regular phantom black hole as photons couple to Weyl tensor*, Eur. Phys. J. C **76**, 594 (2016).

[47] Z. Younsi, A. Zhidenko, L. Rezzolla, R. Konoplya and Y. Mizuno, *A new method for shadow calculations: application to parameterised axisymmetric black holes*, Phys. Rev. D **94**, 084025 (2016), arXiv:1607.05767.

[48] A. Abdujabbarov, M. Amir, B. Ahmedov, S. Ghosh, *Shadow of rotating regular black holes*, Phys. Rev. D **93**, 104004 (2016).

[49] A. Abdujabbarov, L. Rezzolla, B. Ahmedov, *A coordinate-independent characterization of a black hole shadow*, Mon. Not. R. Astron. Soc. **454**, 2423 (2015).

[50] F. Atamurotov, B. Ahmedov, A. Abdujabbarov, *Optical properties of black hole in the presence of plasma: shadow*, Phys. Rev D **92**, 084005 (2015).

[51] A. Abdujabbarov, F. Atamurotov, N. Dadhich, B. Ahmedov, Z. Stuchlík, *Energetics and optical properties of 6-dimensional rotating black hole in pure Gauss-Bonnet gravity*, Eur. Phys. J. C **75**, 399 (2015).

[52] F. Atamurotov, A. Abdujabbarov, B. Ahmedov, *Shadow of rotating non-Kerr black hole*, Phys. Rev D **88**, 064004

(2013).

[53] N. Tsukamoto, *Black hole shadow in an asymptotically-flat, stationary, and axisymmetric spacetime: the Kerr-Newman and rotating regular black holes*, Phys. Rev D **97**, 064021 (2018), arXiv:1708.07427.

[54] P. V. P. Cunha1, C. A. R. Herdeiro, *Shadows and strong gravitational lensing: a brief review*, Gen.Rel.Grav. **50** no.4, 42 (2018), arXiv:1801.00860.

[55] S. W. Wei, Y. X. Liu, and R. B. Mann, *Intrinsic curvature and topology of shadow in Kerr spacetime*, Phys. Rev. D **99**,041303 (2019),arXiv:1811.00047.

[56] S. W. Wei, Y. C. Zou, Y. X. Liu, and R. B. Mann, *Curvature radius and Kerr black hole shadow*, arXiv:1904.07710.

[57] R. A. Konoplya, *Shadow of a black hole surrounded by dark matter*, Phys. Lett. B **795**, 1 (2019), arXiv:1905.00064.

[58] R. Roy and U. A. Yajnik, *Evolution of black hole shadow in the presence of ultralight bosons*, arXiv:1906.03190.

[59] B. C. Xanthopoulos, *Metric and electromagntic perturbations of the Reissner-Nordström black hole*, Proc. R. Soc. A **378** 73 (1981).

[60] P. S. Letelier and W. M. Vieira, *Chaos in black holes surrounded by gravitational waves*, class. Quantum Grav. **14** 1249-1257 (1997).